Ma *et al.*
European Journal of Medical Research (2024) 29:495
https://doi.org/10.1186/s40001-024-02093-y

European Journal of Medical Research

RESEARCH

Open Access

Identification of cuproptosis-related genes in Alzheimer's disease based on bioinformatic analysis

Ming-ming Ma[1], Jing Zhao[1], Ling Liu[2] and Cai-ying Wu[1*]

Abstract

Objective To explore the role of cuproptosis in Alzheimer's disease (AD).

Methods An AD-related microarray dataset was downloaded from the Gene Expression Omnibus (GEO) database (GSE140830). Weighted gene co-expression network analysis was used to identify AD-related modular genes. The Venn analysis was performed to obtain module genes associated with apoptosis and cuproptosis. Besides, we conducted an enrichment analysis of overlapped genes and constructed the protein–protein interaction (PPI) network, followed by screening hub genes and those significantly associated with AD were used to construct models of apoptosis and cuproptosis, respectively. Further, receiver operating characteristic (ROC) curve analysis, decision curve analysis (DCA), and subgroup analysis were used to compare the AD prediction performance of two models. Finally, the accuracy and reliability of AD prediction models were verified by GSE26927.

Results We obtained 42 module genes related to apoptosis and 9 module genes related to cuproptosis. The enrichment analysis results revealed MAPK signaling pathway as the common signaling pathway of apoptosis- and cuproptosis-related genes. Next, the hub genes associated with apoptosis (TRADD, FADD, BIRC2, and CASP2) and cuproptosis (MAP2K1, SLC31A1, and PDHB) in AD were identified, which were used to construct apoptosis and cuproptosis models to distinguish AD patients from the control group ($P < 0.05$). The ROC, DCA, and subgroup analysis results showed that apoptosis-related models and cuproptosis-related models had comparable ability in predicting AD. GSE26927 further confirmed that the two models have comparable predictive effects for AD.

Conclusions The cuproptosis model had a certain performance in predicting AD. Three hub genes (MAP2K1, SLC31A1, and PDHB) closely related to cuproptosis in AD might serve as biomarkers for AD diagnosis and treatment.

Keywords Alzheimer's disease, Bioinformatics, Cuproptosis, Apoptosis

Introduction

Alzheimer's disease (AD) is a neurodegenerative disorder characterized by cognitive decline and memory impairment, which represents the primary manifestation of dementia [1, 2]. With the continuous development of the economy, the continuous improvement of people's living standards, and the intensification of population aging, AD has become an international public health problem, which brings a huge burden to families and society, and seriously affects the quality of life of patients [3]. Despite the multitude of hypotheses proposed by researchers

*Correspondence:
Cai-ying Wu
wcy850502@126.com
[1] Neurology, Hangzhou Red Cross Hospital, No. 208, East Huan Cheng Road, Gongshu District, Hangzhou 310003, Zhejiang, China
[2] Gastroenterology, The Second Affiliated Hospital Zhejiang University School of Medicine (City East Campus), Hangzhou 310021, Zhejiang, China

regarding the etiology of AD, none have proven entirely satisfactory in elucidating its underlying mechanisms [4].

Apoptosis, an intricate and regulated mechanism of cellular demise, is of paramount importance in maintaining cellular equilibrium and optimal functionality [5]. Several investigations have demonstrated the presence of apoptosis in both neurons and glia of AD [6]. The significance of apoptosis in the initiation and progression of AD is well-established and widely acknowledged [5].

Moreover, a novel form of cell death known as cuproptosis has recently emerged, distinguishing itself from other forms of regulated cell death such as oxidative stress-induced death, scorch death, ferroptosis, and necrotic apoptosis [7]. Copper is an essential trace element that is a component of copper proteins involved in a variety of physiological functions, including energy production, connective tissue production, and neurotransmission [8, 9]. Based on pertinent reports, the primary mechanism underlying cuproptosis entails the excessive accumulation of lipid mitochondrial enzymes and the depletion of Fe–S cluster proteins during mitochondrial stress [10]. Furthermore, a substantial body of research has consistently demonstrated that mitochondrial dysfunction plays a crucial role in the progression of AD [11]. Previous studies have shown that metal chelators play an important role in improving metal homeostasis (iron, copper, and zinc), inhibiting Aβ accumulation, inhibiting tau hyperphosphorylation, and relieving neuroinflammation [12]. These revelations open up novel avenues for the therapeutic intervention of AD. Nevertheless, despite the existing association between cuproptosis and the pathogenesis of AD [13], further compelling evidence is required to substantiate this relationship.

Currently, scientists were mainly studying the relationship between cuproptosis and AD from a mechanistic perspective [12]. However, the methodology employed in this study aimed to substantiate the correlation between cuproptosis and AD by contrasting the predictive efficacy of apoptosis models and cuproptosis models on AD.

Materials and methods

Microarray data

The microarray datasets GSE140830 (https://ftp.ncbi.nlm.nih.gov/geo/series/GSE140nnn/GSE140830/matrix/) and GSE26927 (https://ftp.ncbi.nlm.nih.gov/geo/series/GSE26nnn/GSE26927/matrix/) were downloaded from the Gene Expression Omnibus (GEO) database, which were captured by the GPL15988 and GPL6255 platforms, respectively. The principle of inclusion of data sets were that the number of data sets was greater than 100 and the proportion of AD patients to normal samples was similar. Finally, the GSE140830 dataset was used as a training set including 261 AD patients and 281 normal samples. The GSE26927 dataset served as a validation set including 60 AD patients and 55 normal samples.

Weighted gene co-expression network analysis (WGCNA)

Firstly, we removed batch effects from the data and proceeded to the next step of analysis. Second, this study used BiocManger (Version: 1.30.10) in the R suite to download an R package termed WGCNA (Version: 1.70-3), and constructed the gene co-expression network. Subsequently, constructing the adjacency matrix describes the correlation strength between nodes. Then, converted the adjacency matrix to the topological overlap matrix (TOM). The TOM matrix was a method of quantitatively describing the similarity between two nodes by comparing their weighted correlations with other nodes. Next, the hierarchical clustering recognition module included at least 100 genes in each module. Finally, we calculated feature genes, performed hierarchical clustering on modules, and merged similar modules (abline = 0.25).

Identification of apoptosis and cuproptosis-related genes associated with AD

In this study, the pathways with the highest scores associated with apoptosis were selected from the PathCards database (https://pathcards.genecards.org/Search/Results?query=apoptosis), and genes associated with apoptosis were obtained. The genes related to cuproptosis were obtained based on research related literature, including "Pan cancer profiles of the cuproptosis gene set", "The cuproptosis-related signature predicts diagnosis and indicators of the acute microenvironment in breast cancer", and "A novel cuproptosis-related LncRNA signature to predict prognosis in hepatocellular carcinoma" [14–16]. Research overlapped these genes with the AD-related module genes in WGCNA. The study used a Venn diagram constructed by the ggVennDiagram package of R software to represent the details of overlapped genes.

Functional enrichment analysis of overlapped genes

We used the R software clusterProfiler package and the org.Hs.eg.db package for gene ontology (GO) and the Kyoto Encyclopedia of Genes and Genomes (KEGG) for overlapped gene enrichment analysis. The GO terms comprised three divisions: biological process (BP), cellular component (CC), and molecular function (MF). The KEGG database contained pathway datasets related to biological functions, diseases, chemicals, and drugs.

Protein–protein interaction (PPI) network establishment and identification of hub genes

The study used the online tool Search Tools for Retrieval of Interacting Genes (STRING) (https://cn.string-db.

org/) to analyze protein interactions between apoptosis-related overlapped genes and cuproptosis-related overlapped genes. Hub genes in apoptosis overlapped genes were screened using the CytoHubba plug-in in Cytoscape (Version 3.9.0). The importance of nodes was evaluated by Degree, Closeness, and Between, and the top 10 nodes were selected. Then, the screened hub genes were common nodes. Finally, the PPI network was constructed to visualize the hub genes related to apoptosis and the hub genes related to cuproptosis.

Construction and evaluation of the nomogram model

To obtain the hub genes that can better distinguish AD patients from the control group, we used multivariate logistic regression analysis to screen the hub genes associated with apoptosis and the hub genes associated with cuproptosis that were significantly associated with AD. Next, we used the ggplot2 package of R software to build nomograms and calibration curves associated with hub genes for predicting AD patients. Furthermore, the AD prediction model was constructed based on the hub genes. The performance of the models in predicting AD was evaluated using receiver operating characteristic (ROC) curve analysis constructed by the pROC package of R and decision curve analysis (DCA) constructed by the rmda package of R.

Subgroup analysis

To further study the performance of the models in predicting AD, subgroup analysis was conducted on samples based on gender and age. The ROC curve and DCA were used to compare the performance of the apoptosis model and cuproptosis model in predicting AD.

To more comprehensively compare the differences between apoptosis and cuproptosis models in predicting AD. We included age and sex, two clinical factors of significant value, into multivariate logistic regression analysis. Moreover, we incorporated clinical features that were significantly associated with AD into the model and established a new predictive model. Besides, the predictive performance of the model was compared using ROC curve analysis and DCA.

External validation of the model efficacy

To verify the clinical efficacy of the models, we identified the performance of apoptosis model and cuproptosis model in predicting AD using the GSE26927 dataset by ROC curves and DCA. Secondly, subgroup analysis was performed according to age and sex to further evaluate the predictive efficacy of the two models.

Statistical analysis

We used R language (Version 3.6.3) for bioinformatics analysis and SPSS 25.0 software for statistical analysis of the data. Sensitivity, specificity, accuracy, positive predictive value (PPV), negative predictive value (NPV), positive likelihood ratio (PLR), and negative likelihood ratio (NLR) were determined. The goodness of fit for models were assessed by the Hosmer–Lemeshow test. Area under the curve (AUC) calculation was carried out for comparing cuproptosis-related model and apoptosis-related model. DCA determined the usefulness of the model by evaluating the net benefit under different threshold probabilities. $P<0.05$ was deemed statistically significant.

Results

Weighted co-expression network construction and identification of core modules

To select core models related to AD, we performed WGCNA. The Pearson correlation coefficient was used to cluster GSE140830 samples and removed outliers. When the soft threshold was 6 ($R^2=0.86$), the scale-free network was constructed (Fig. 1A, B). Then, the adjacency matrix was established and the TOM was constructed. According to the different expression types of genes, 19 co-expression modules were ultimately obtained (Fig. 1C). The study analyzed the correlation between characteristic genes and phenotype in the modules and ultimately found that three modules were associated with AD. These three modules included the magenta module (508 genes) (Cor = 0.15, $P=5.7e{-}4$), the cyan module (266 genes) (Cor = −0.11, $P=7.6e{-}3$), and the blue module (3081 genes) (Cor = −0.11, $P=0.01$) (Fig. 1D).

In this study, 185 apoptosis-related genes were downloaded from the Pathway database, and 44 cuproptosis-related genes were collected from the article. Venn diagram showed that there were 42 apoptosis-related overlapped genes in the intersection of the blue module and apoptosis-related genes, and 9 cuproptosis-related overlapped genes in the intersection of the blue module and cuproptosis-related genes (Fig. 2A, B). There were 6 apoptosis-related overlapped genes in the intersection of the cyan module and apoptosis-related genes, and 1 cuproptosis-related overlapped genes in the intersection of the cyan module and cuproptosis-related genes (Fig. 2C, D). There were 5 apoptosis-related overlapped genes at the intersection of the magenta module and apoptosis-related genes, but there was no cuproptosis-related overlapped gene intersection between the magenta module and cuproptosis-related genes (Fig. 2E, F). Based on the above results, the overlapped genes of blue module and apoptosis-related genes and the

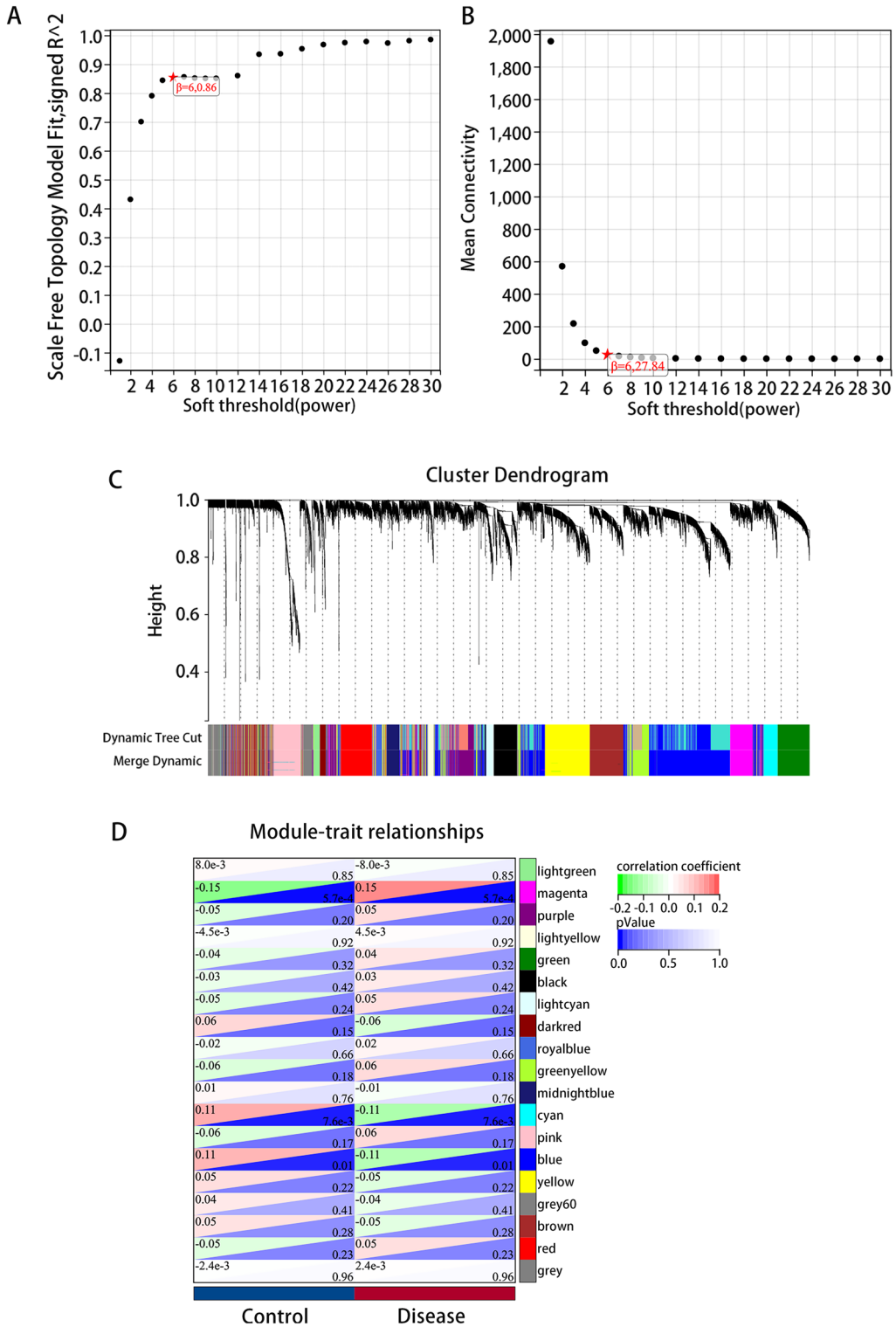

Fig. 1 The results of weighted gene co-expression network analysis (WGCNA). **A** Analysis of the scale-free index for various soft-threshold powers (β). **B** Analysis of the mean connectivity for various soft-threshold powers. **C** WGCNA module picture, the upper part of the tree represents the initial module, while the lower part represents the final module. Different colors represent different modules, while gray represents unclassified genes. **D** WGCNA module and clinical phenotype correlation diagram, behavior module, column clinical phenotype

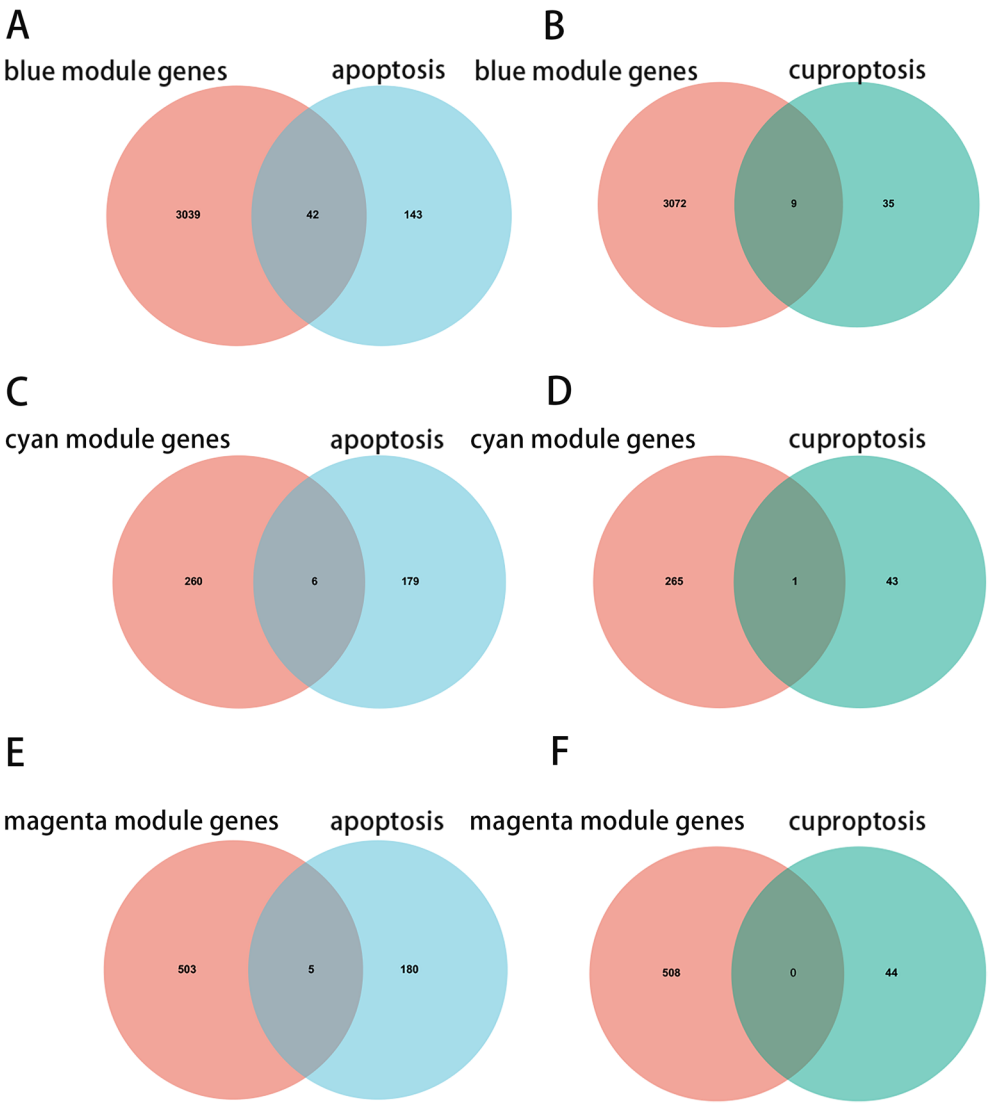

Fig. 2 Venn diagram showing the number of AD-related module genes and apoptosis-related genes, as well as genes that overlap with cuproptosis-related genes. **A**,**B** Venn diagram of blue module genes and apoptosis genes, as well as blue module genes and cuproptosis genes. **C**,**D** Venn diagram of cyan module genes and apoptosis genes, as well as cyan module genes and cuproptosis genes. **E**,**F** Venn diagram of magenta module genes and apoptosis genes, as well as magenta module genes and cuproptosis genes

overlapped genes of blue module and cuproptosis-related genes were selected for further analysis.

Enrichment analysis of overlapped genes

To investigate the possible pathways of the apoptosis gene set and cuproptosis gene set, we performed a function enrichment analysis. The GO analysis results (including BP, CC, and MF) of 42 apoptosis-related overlapped genes are reflected in Fig. 3A. The results showed that overlapped genes were mainly concentrated in cell death, apoptotic process, and regulation of cell death. The results of the KEGG pathway analysis indicated that overlapped genes involved in apoptosis, NOD-like receptor signaling pathway, apoptosis-multiple species, p53 signaling pathway, and MAPK signaling pathway (Fig. 3B).

The GO analysis of 9 overlapped genes related to cuproptosis exhibited that overlapped genes were closely related to metal ion transport, copper ion transport, and cuproptosis (Fig. 3C). The KEGG pathways that overlapped genes involved in included prion diseases, HIF-1 signaling pathway, apoptosis, and MAPK signaling pathway (Fig. 3D).

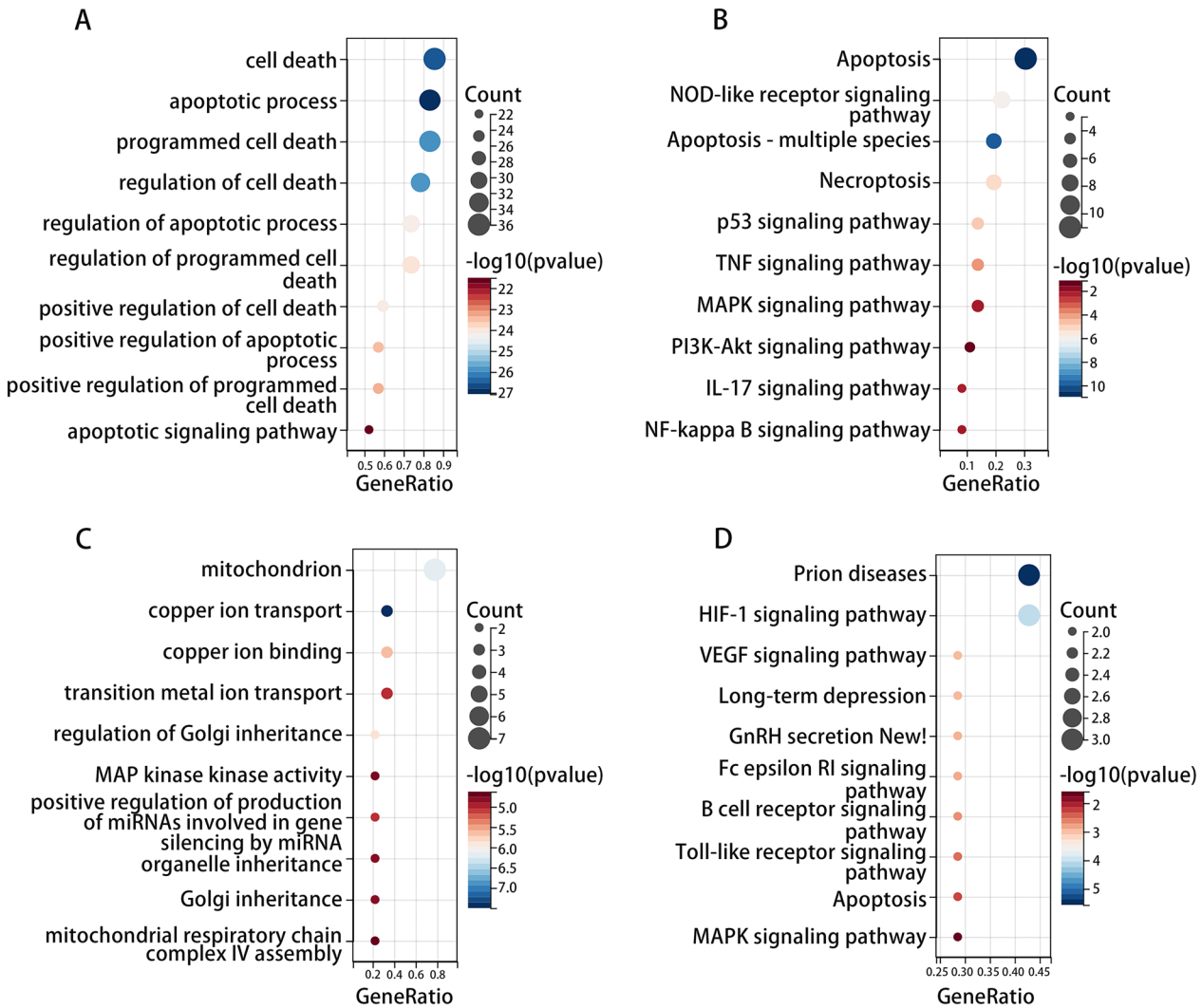

Fig. 3 Enrichment analysis of overlapped genes. **A** Gene ontology (GO) analysis of apoptosis-related overlapped genes. **B** Analysis of Kyoto Encyclopedia of Genes and Genomes (KEGG) pathway of apoptosis-related overlapped genes. **C** GO analysis of cuproptosis-related overlapped genes. **D** KEGG pathway analysis of cuproptosis-related overlapped genes

PPI network construction and hub gene identification

To screen for apoptosis genes related to AD, the study used CytoHubba in Cytoscape to calculate the closeness, betweenness, and degree between various proteins and ranked them according to their correlation. The study selected the first 10 genes to cross, and finally, 8 overlapped genes were obtained, including BCL2, BIRC2, CASP1, CASP2, CASP3, CASP9, FADD, and TRADD (Fig. 4A). PPI analysis was performed on 8 apoptosis-related hub genes and 9 cuproptosis-related hub genes using the STRING database. Finally, the pivotal genes related to apoptosis and cuproptosis were visualized using Cytoscape (Fig. 4B, C).

Construction and evaluation of the nomogram model

To explore the predictive efficacy of the hub genes, we first performed multivariate logistic regression analysis. As shown in Table 1, apoptosis hub genes including TRADD, FADD, BIRC2, and CASP2 were significantly related to AD ($P<0.05$), which were used for apoptosis model construction and visualized by nomogram (Fig. 5A). Calibration curve results showed that nomogram predictions showed an agreement with the actual observations (Fig. 5B). ROC curve (AUC = 0.638) and DCA results exhibited that the apoptosis model had good performance in predicting AD (Fig. 5C, D).

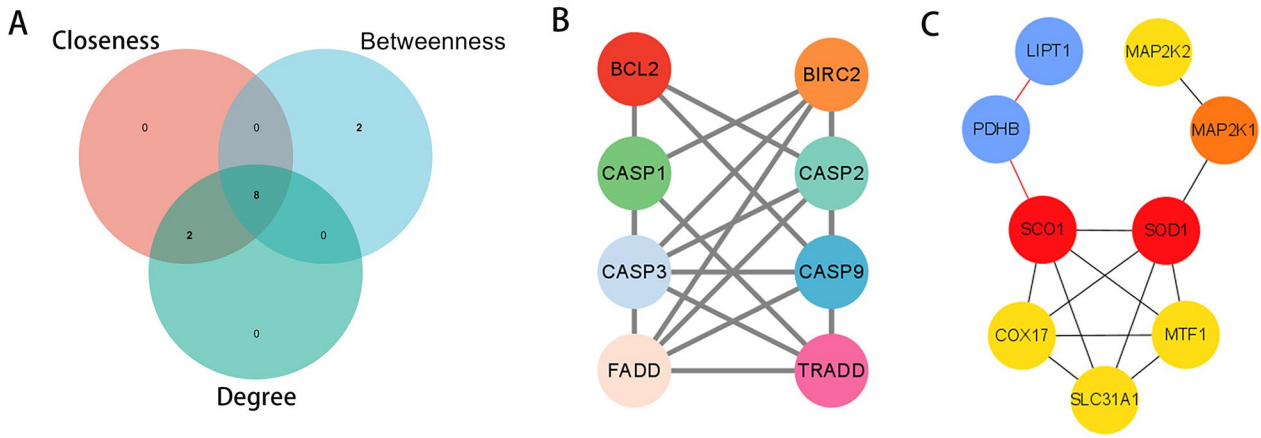

Fig. 4 Construction of protein–protein interaction (PPI) network. **A** Screening of apoptosis-related overlapped genes according to the criteria. **B** PPI network construction of apoptosis-related hub genes. **C** PPI network construction of cuproptosis-related hub genes

Table 1 Multivariate logistic regression analysis of apoptosis hub genes

Characteristics	Total (*N*)	Odds ratio (95% CI)	*P* value
CASP3	542	0.594 (0.221–1.599)	0.303
CASP9	542	0.173 (0.014–2.058)	0.165
TRADD	542	4.529 (1.696–12.095)	0.003
FADD	542	7.930 (2.269–27.717)	0.001
BIRC2	542	3.537 (1.550–8.074)	0.003
CASP2	542	2.841 (1.398–5.773)	0.004
BCL2	542	0.878 (0.441–1.750)	0.712
CASP1	542	0.566 (0.317–1.009)	0.054

N number, *95% CI* 95% confidence interval

Meanwhile, the multivariate logistic regression analysis results of the module genes related to cuproptosis revealed that MAP2K1, SLC31A1, and PDHB were notably associated with AD ($P<0.05$) (Table 2). These three genes were used to cuproptosis model establishment and demonstrated by nomogram (Fig. 6A). Calibration curve results showed that nomogram predictions showed an agreement with the actual observations (Fig. 6B). The results of the ROC curve (AUC = 0.576) and DCA represented that the cuproptosis model had a certain predictive effect on AD (Fig. 6C, D). However, the AUCs between two groups were not statistically different ($P=0.055$) (Table 3).

Subgroup analysis

To further evaluate the efficacy between the apoptosis model and the cuproptosis model in predicting AD, we performed the subgroup analysis. In participants aged ≤65 or male sex, the results of the ROC curve and DCA revealed that the efficacy of the apoptosis model in predicting AD was not significantly different from that of the cuproptosis model ($P>0.05$) (Fig. 7A, C, E, G; Table S1). In those with age >65 or sex female, the performance of the apoptosis model in predicting AD was higher than that of the cuproptosis model ($P<0.05$) (Fig. 7B, D, F, H; Table S1).

External validation of the model efficacy

To further explore the accuracy and reliability of the model, the performance of the apoptosis model and cuproptosis model in predicting AD was verified in the GSE26927 dataset. ROC curve and DCA results exhibited that the apoptosis model and cuproptosis model had certain ability in predicting AD, and there was no significant difference between the two models (Fig. 8A, B; Table 4). In the age ≥65, male and female subgroups, the apoptosis model had no significant difference in predicting AD compared with the cuproptosis model ($P>0.05$) (Fig. 8D–F, H–J; Table S2). However, cuproptosis model had higher predictive ability of AD than apoptosis model in the age <65 group ($P<0.05$) (Fig. 8C, G; Table S2).

Gene–clinical model construction

To further explore the difference between the apoptosis model and cuproptosis model in predicting AD, we combined clinical features associated with AD to construct new predictive models. TRADD, FADD, BIRC2, CASP2, and age were significantly related to AD, which was used for the construction of the apoptosis-clinical model ($P<0.05$) (Table S3). MAP2K1, PDHB, PDHB, and age were significantly related to AD, which was used for the construction of the cuproptosis-clinical model ($P<0.05$) (Table S4). The ROC curve and DCA indicated that the ability of the apoptosis-clinical model and cuproptosis-clinical model to predict AD was similar ($P=0.116$) (Fig. 9A, B; Table S5).

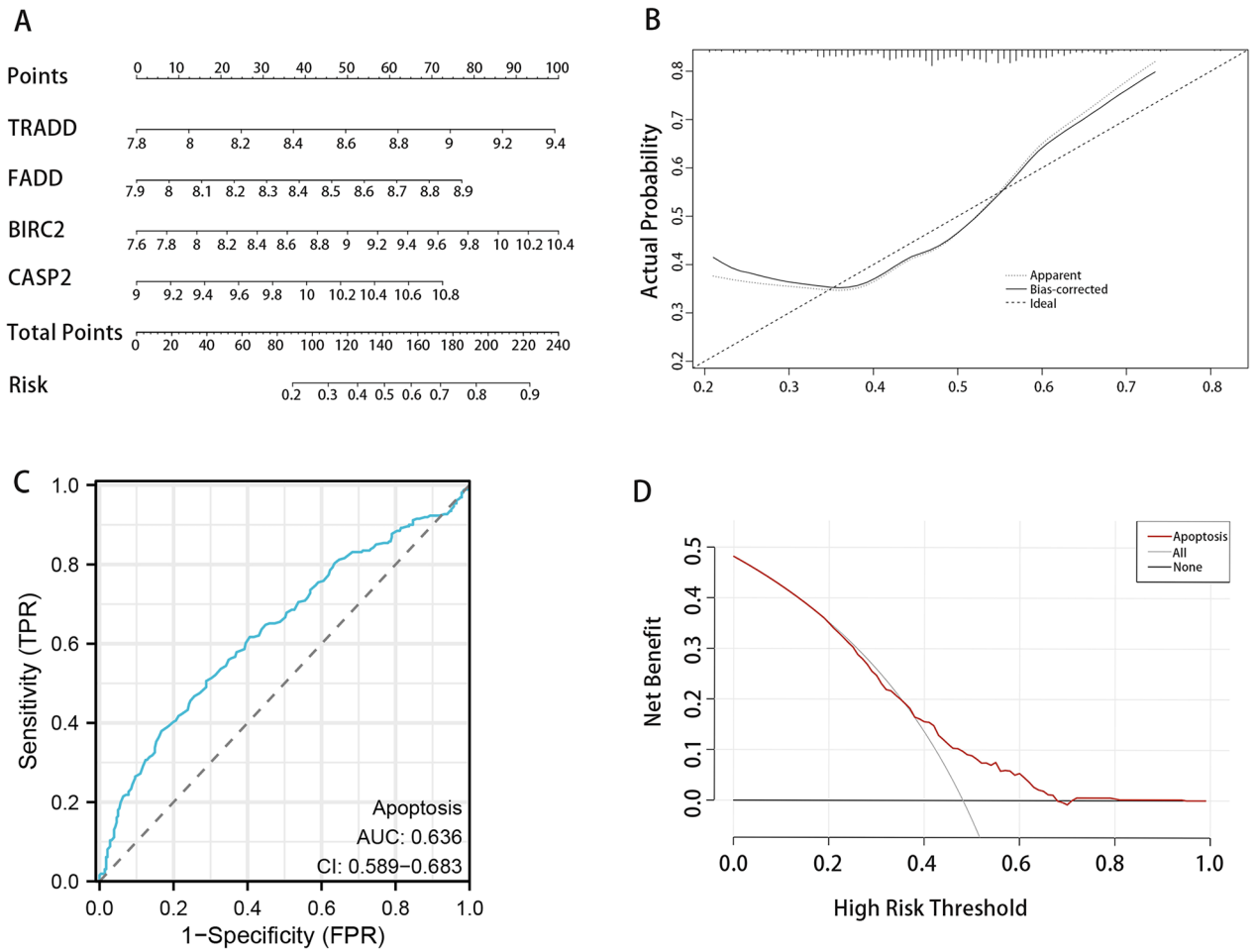

Fig. 5 The efficiency of a model constructed from apoptosis-related hub genes in predicting AD. **A** The nomogram predicts the occurrence of AD, which includes apoptotic genes TRADD, FADD, BIRC2, and CASP2. **B** Calibration curve of the nomogram. **C**,**D** ROC curve analysis and DCA were used to evaluate the prediction performance of the apoptosis gene model. TPR, true positive rate; FPR, false positive rate; AUC, area under the curve; CI, confidence interval

Table 2 Multivariate logistic regression analysis of cuproptosis hub genes

Characteristics	Total (*N*)	Odds ratio (95% CI)	*P* value
COX17	542	0.828 (0.361–1.898)	0.655
LIPT1	542	0.138 (0.009–2.226)	0.163
MAP2K1	542	3.843 (1.466–10.073)	0.006
MAP2K2	542	1.154 (0.548–2.429)	0.706
MTF1	542	1.880 (0.659–5.363)	0.238
PDHB	542	0.279 (0.105–0.738)	0.010
SCO1	542	0.329 (0.028–3.807)	0.374
SLC31A1	542	0.025 (0.112–0.017)	0.025
SOD1	542	1.600 (0.787–3.250)	0.194

N number, *95% CI* 95% confidence interval

Discussion

AD is a neurodegenerative disorder characterized by cognitive decline and memory impairment, significantly compromising individuals' occupational and daily functioning [17, 18]. Lesion marker of AD includes β-amyloid plaque precipitation and neuronal fiber entanglement of hyperphosphorylated tau [19]. Cuproptosis, a novel form of cellular demise, has been recently unveiled through scientific inquiry [20, 21]. Research has shown a correlation with the occurrence of AD, but there is no direct evidence to prove it. Consequently, this study aims to delve deeper into the role of cuproptosis in the assessment of prognosis and treatment of AD patients.

The study used the GEO database to obtain data on a total of 542 samples, including 261 patients with AD and 281 normal samples. Additionally, three module gene sets associated with AD were procured through the application of WGCNA. Subsequently, a total of 44

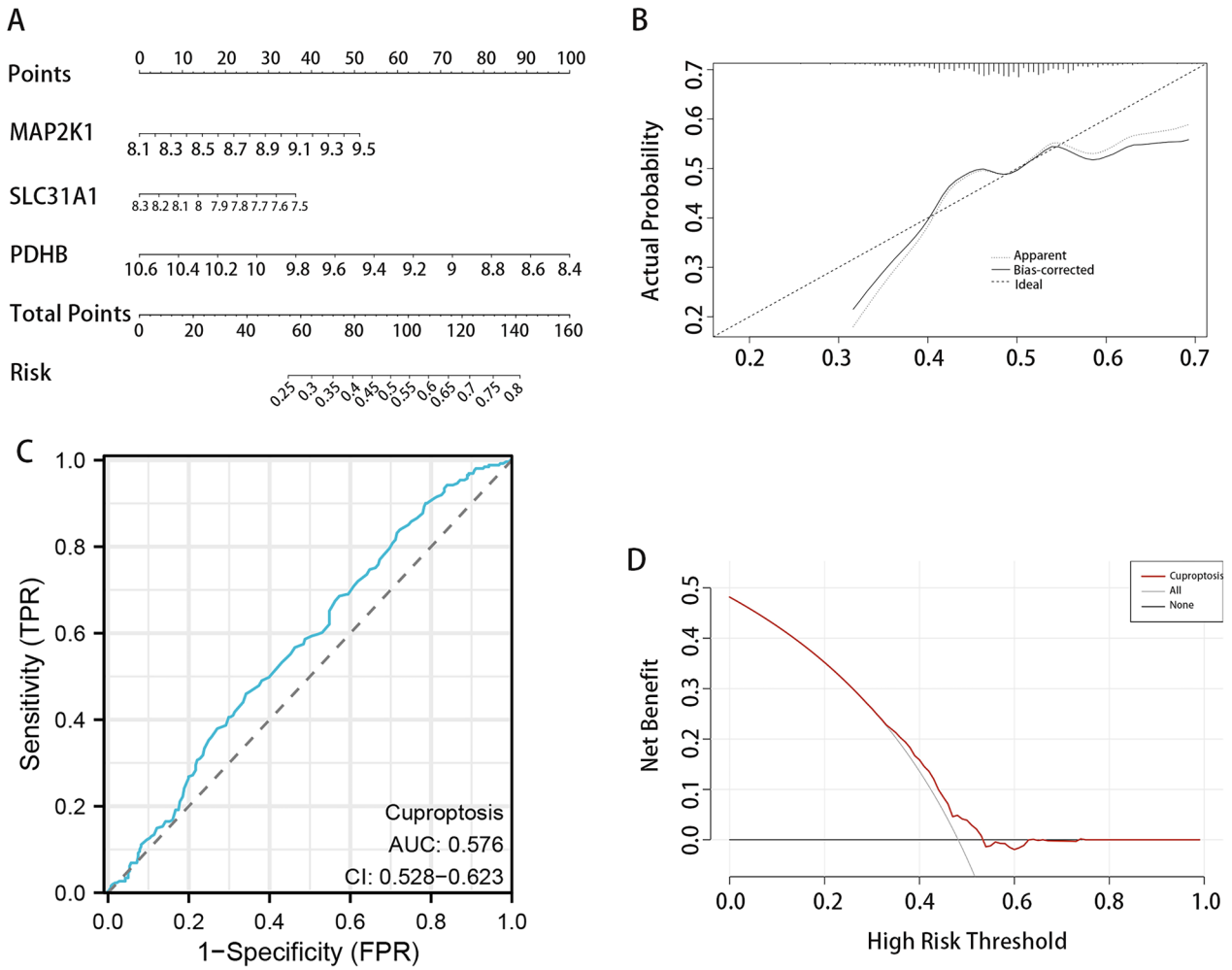

Fig. 6 The efficiency of a model constructed from cuproptosis-related hub genes in predicting AD. **A** The nomogram predicts the occurrence of AD, and the genes responsible for cuproptosis in the column chart include MAP2K1, SLC31A1, and PDHB. **B** Calibration curve of the nomogram. **C**,**D** ROC curve analysis and DCA of the cuproptosis model. TPR, true positive rate; FPR, false positive rate; AUC, area under the curve; CI, confidence interval

Table 3 ROC curve analysis of two prediction models

	AUC	95% CI	Specificity	Sensitivity	Accuracy	*P* value
All samples						
Apoptosis	0.636	0.589–0.683	0.506	0.712	0.612	0.055
Cuproptosis	0.576	0.528–0.623	0.460	0.658	0.563	

AUC area under the curve, *95% CI* 95% confidence interval

genes associated with apoptosis and 9 genes associated with cuproptosis were identified through the intersection of the apoptosis gene set, the cuproptosis gene set, and three AD-related module gene sets.

Based on the results of the enrichment analysis of overlapped genes, we found that the MAPK signaling pathway was closely related to apoptosis and cuproptosis. Previous research has demonstrated that cadmium can induce apoptosis in retinal pigment epithelium cells by activating the MAPK signaling pathway [22]. There were also studies indicating that the MAPK signaling pathway is involved in DSF/Cu induced death in cancer [23]. This pathway and other factors had been reported to cause Aβ and hyperphosphorylated tau proteins to aggregate in

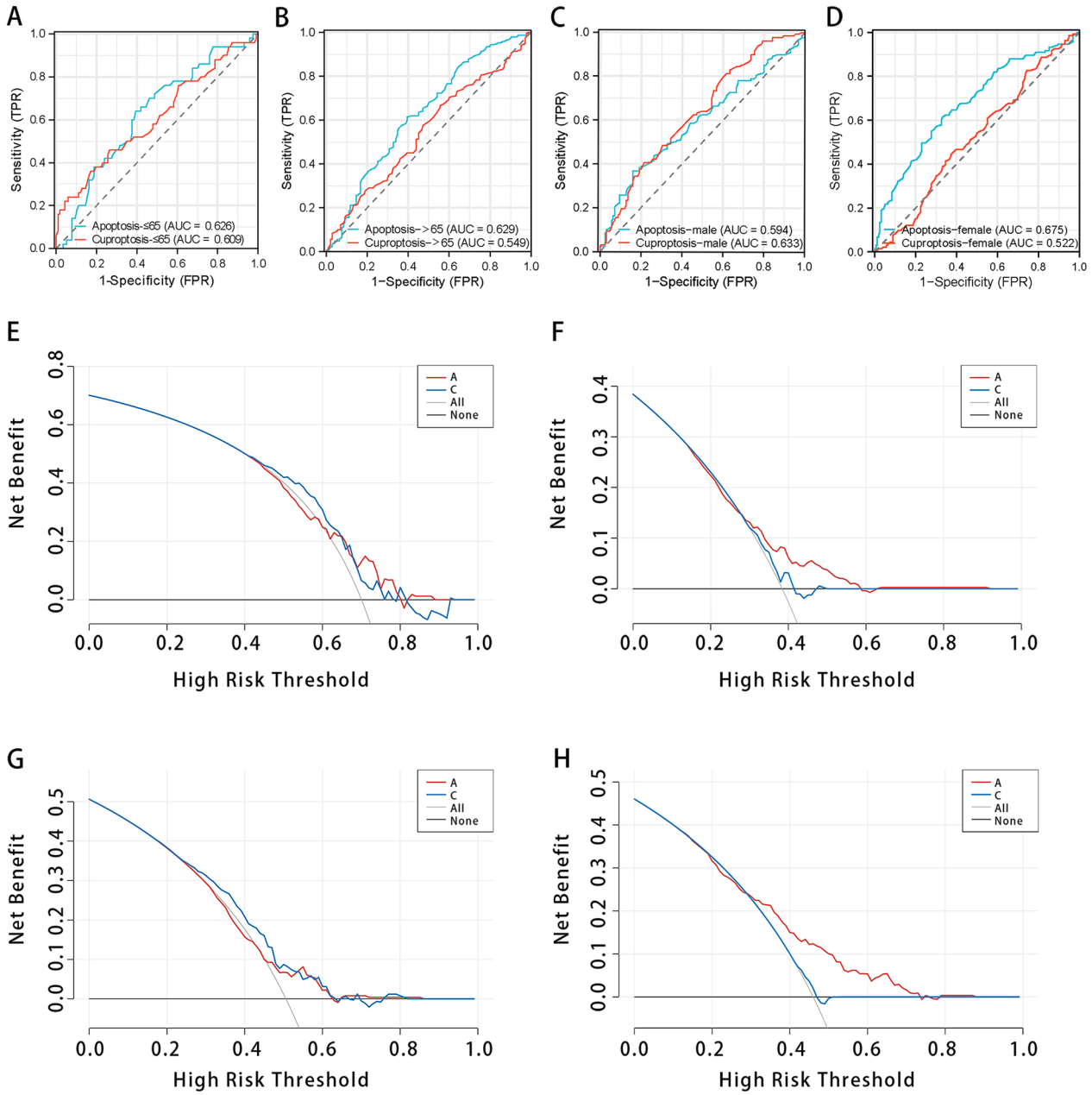

Fig. 7 The performance of the apoptosis model and cuproptosis model in predicting AD in different subgroups. **A**–**D** ROC curve of AD predicted by the apoptosis model and cuproptosis model in each clinical subgroup. **E**–**H** The DCA of AD was predicted by the apoptosis model and cuproptosis model in each clinical subgroup. TPR, true positive rate; FPR, false positive rate; AUC, area under the curve; CI, confidence interval; A, apoptosis; C, cuproptosis

the brain and induce neuronal apoptosis in AD [24, 25]. Based on the previous research, it can be inferred that there is a connection between the mechanisms of apoptosis and cuproptosis in the progression of AD.

Through multivariate logistic regression analysis, four apoptosis-related hub genes (TRADD, FADD, BIRC2, and CASP2) and three cuproptosis-related hub genes (MAP2K1, SLC31A1, and PDHB) were identified. Subsequently, this study examined the potential mechanisms of action of each hub gene in cuproptosis in AD. MAP2K1 is an important member of the mitogen-activated protein kinase family, also known as MEK1, which plays a role in cell proliferation and apoptosis. In hepatocellular carcinoma, miR-539 could directly target and regulate

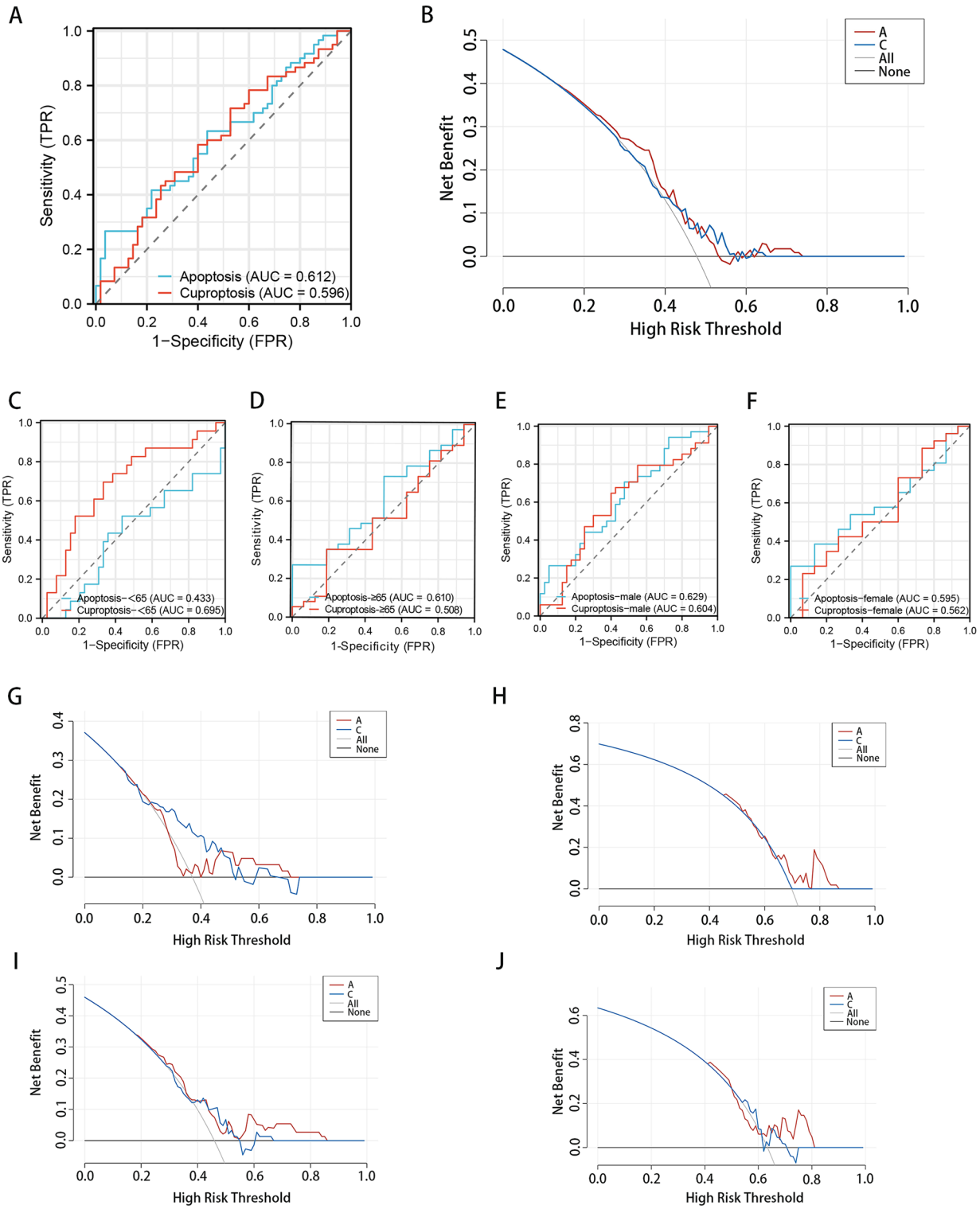

Fig. 8 External validation of the apoptosis model and cuproptosis model. **A**,**B** ROC curves and DCA of apoptosis model and cuproptosis model in GSE26927. **C**–**F** The models predicted the ROC curve of AD in each clinical subgroup. **G**–**J** The models predicted the DCA of AD in each clinical subgroup. TPR, true positive rate; FPR, false positive rate; AUC, area under the curve; CI, confidence interval; A, apoptosis; C, cuproptosis

Table 4 ROC curve analysis of two prediction models in GSE26927

	AUC	95%	Specificity	Sensitivity	Accuracy	*P* value
All samples						
Apoptosis	0.612	0.509–0.714	0.267	0.964	0.600	0.857
Cuproptosis	0.596	0.492–0.701	0.717	0.473	0.600	

AUC area under the curve, *95% CI* 95% confidence interval

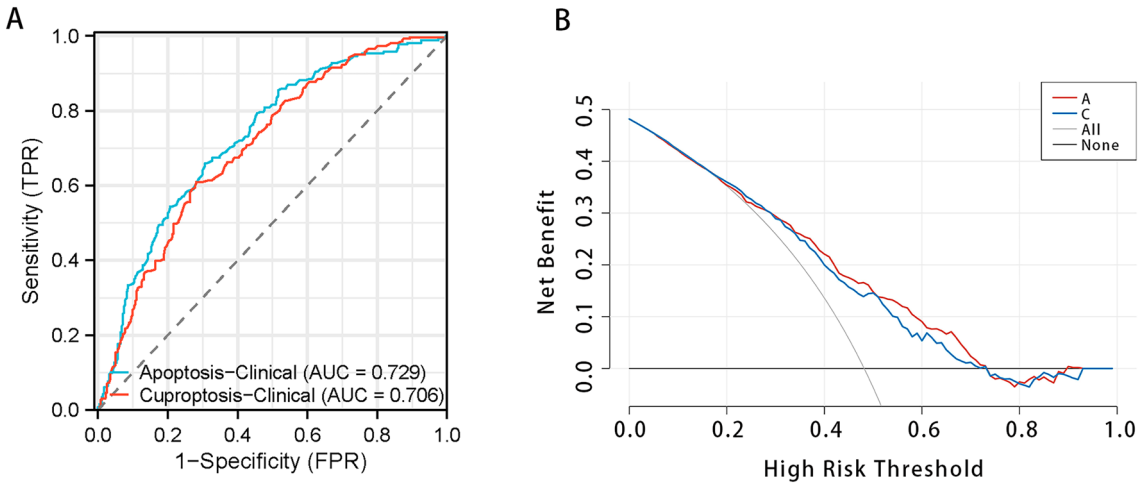

Fig. 9 Comparison of apoptosis and cuproptosis models in predicting AD performance after incorporating clinical features. **A** Two models predict AD's ROC curve analysis. **B** Two models predict the DCA of AD. TPR, true positive rate; FPR, false positive rate; AUC, the area under the curve. AUC, area under the curve; 95% CI, 95% confidence interval

MAP2K1 to inhibit the proliferation, migration, and invasion of hepatocellular carcinoma, and promote cell apoptosis [26]. In gastric cancer, miRNA-34c-5p inhibited the proliferation, migration, and invasion of gastric cancer cells through MAP2K1 [27]. Studies in AD have exhibited that trametinib can increase autophagic lysosomal activity through TFEB activation, thereby inhibiting MEK, thereby protecting neurons from Aβ loading [28]. SCL31A1 encodes the copper transporter Ctr1, which is a fundamental player in the maintenance of human copper homeostasis. Pan-cancer analysis of SLC31A1 indicated that it plays a key role in lung, stomach, kidney, and colorectal cancers [29]. Studies related to fruit flies have shown that inhibiting Ctr1 in the nervous system of drosophila can effectively improve Aβ42-induced Alzheimer's disease-like symptoms [30]. Pyruvate dehydrogenase E1 subunit beta (PDHB) is a cuproptosis acid gene located in mitochondria that converts pyruvate to acetyl coenzyme A. Studies on colon cancer have shown that miR-146b-5p can directly target PDHB, thereby participating in regulating the growth, invasion, and metabolism of colon cancer cells [31]. In clear cell renal cell carcinoma, low PDHB expression was strongly associated with an increased risk of tumor progression in clear cell renal cell carcinoma [32]. Furthermore, a discernible correlation between PDHB and AD was also identified [33]. Therefore, it can be inferred that the pivotal gene in the cuproptosis model exhibits a strong connection with AD.

Studies have exhibited that the change of copper homeostasis is closely related to the pathogenesis of AD, and copper may interact with the pathogenic factors of Aβ and tau [20]. Copper can also directly bind to Aβ peptides, thereby increasing the aggregation of Aβ and enhancing neurotoxicity [34]. In addition, in AD patients, copper may play a pathogenic role in tau proteins, such as triggering phosphorylation and clustering of tau proteins, thereby enhancing the neurotoxicity of tau aggregates [35, 36]. Thus, cuproptosis might be related to the progression of AD via interacting with Aβ and regulating tau proteins.

Apoptosis model and cuproptosis model were developed to predict AD based on hub genes. The findings from the nomogram, calibration curve, ROC curve analysis, and DCA consistently demonstrated that both the apoptosis model and cuproptosis model exhibited comparable efficacy in predicting AD, which was validated by the GSE26927 dataset. To verify this conclusion, the model further combined clinical features of

age, and the results indicated that the performance of the new apoptosis model and the new cuproptosis model in predicting AD was also comparable. The investigation of relevant literature indicates that apoptosis is closely related to the occurrence and development of AD [6]. In summary, the research results further confirm the crucial role of cuproptosis in the occurrence and development of AD.

This study has some advantages. First, the innovation of this paper is to compare the efficacy of cuproptosis-related model and apoptosis-related model in predicting AD by constructing multiple models and subgroup analysis, so as to prove the value of copper death in AD. Second, we construct a cuproptosis model with good performance in predicting AD. Third, we identified MAP2K1, SLC31A1, and PDHB as potential biomarkers for AD. This study exhibits certain limitations. First, when the two modules with the strongest correlation with AD intersected with the apoptosis gene set and the cuproptosis gene set, it was found that the number of overlapped genes was too small to continue the analysis. Therefore, the study selected modules with a weaker correlation with AD for further analysis. Secondly, the gene set related to cuproptosis is derived from existing research findings, and there are still more genes to be discovered. Thirdly, there is a lack of experimental validation, and relevant experiments are needed to further validate the research results of this article. Since the broader populations might be as the factors such as age, genetic diversity, and disease severity can influence the generalizability of prediction models, the insufficient sample size of this study will lead to the limitation of the applicable population of the model. Therefore, the findings should be verified in a larger cohort.

Conclusion

In conclusion, cuproptosis plays a very important role in the progression of AD, providing a more direct theoretical basis for the treatment of AD. The hub genes associated with cuproptosis can serve as biomarkers for diagnosing and treating AD.

Supplementary Information

The online version contains supplementary material available at https://doi.org/10.1186/s40001-024-02093-y.

Additional file 1.

Additional file 2.

Additional file 3.

Additional file 4.

Additional file 5.

Author contributions

(I) Conception and design: MMM and JZ. (II) Collection and assembly of data: MMM, LL. (III) Data analysis and interpretation: MMM and CYW. (IV) Manuscript writing: All authors. (V) Final approval of manuscript: All authors.

Funding

This work was supported by the following grants: Mechanistic study of HMGN3-m6A modification mediated by WTAP dysregulation in cognitive impairment in patients with tuberculous meningitis [No. 2024KY1358].

Availability of data and materials

The datasets used and/or analyzed during the current study are available from the corresponding authors upon reasonable request.

Declarations

Ethics approval and consent to participate

The Ethics Committee of the Hangzhou Red Cross Hospital agreed to submit the study for review and have waived the need for ethical approval.

Consent for publication

Not applicable.

Competing interests

The authors declare no competing interests.

Received: 26 March 2024 Accepted: 30 September 2024
Published online: 12 October 2024

References

1. Rostagno AA. Pathogenesis of Alzheimer's disease. Int J Mol Sci. 2022;24(1):107.
2. Passeri E, Elkhoury K, Morsink M, Broersen K, Linder M, Tamayol A, et al. Alzheimer's disease: treatment strategies and their limitations. Int J Mol Sci. 2022;23(22):13954.
3. Ren R, Qi J, Lin S, Liu X, Yin P, Wang Z, et al. The China Alzheimer report 2022. Gen Psychiatr. 2022;35(1): e100751.
4. Piekarczyk B, Winiarska-Majczyno M, Pietrzak-Bilinska B, Zadurska M. Assessment of dental arch contact in children without malocclusion aged 3 years. Czas Stomatol. 1988;41(3):167–72.
5. Sharma VK, Singh TG, Singh S, Garg N, Dhiman S. Apoptotic pathways and Alzheimer's disease: probing therapeutic potential. Neurochem Res. 2021;46(12):3103–22.
6. Wang Y, Chen G, Shao W. Identification of ferroptosis-related genes in Alzheimer's disease based on bioinformatic analysis. Front Neurosci. 2022;16: 823741.
7. Lai Y, Lin C, Lin X, Wu L, Zhao Y, Lin F. Identification and immunological characterization of cuproptosis-related molecular clusters in Alzheimer's disease. Front Aging Neurosci. 2022;14: 932676.
8. Prohaska JR. Role of copper transporters in copper homeostasis. Am J Clin Nutr. 2008;88(3):826S–9S.
9. Lutsenko S, Bhattacharjee A, Hubbard AL. Copper handling machinery of the brain. Metallomics. 2010;2(9):596–608.
10. Oliveri V. Selective targeting of cancer cells by copper ionophores: an overview. Front Mol Biosci. 2022;9: 841814.
11. Tang J, Oliveros A, Jang MH. Dysfunctional mitochondrial bioenergetics and synaptic degeneration in Alzheimer disease. Int Neurourol J. 2019;23(Suppl 1):S5–10.
12. Chen LL, Fan YG, Zhao LX, Zhang Q, Wang ZY. The metal ion hypothesis of Alzheimer's disease and the anti-neuroinflammatory effect of metal chelators. Bioorg Chem. 2023;131: 106301.
13. Gromadzka G, Tarnacka B, Flaga A, Adamczyk A. Copper dyshomeostasis in neurodegenerative diseases-therapeutic implications. Int J Mol Sci. 2020;21(23):9259.
14. Liu H. Pan-cancer profiles of the cuproptosis gene set. Am J Cancer Res. 2022;12(8):4074–81.

15. Li J, Wu F, Li C, Sun S, Feng C, Wu H, et al. The cuproptosis-related signature predicts prognosis and indicates immune microenvironment in breast cancer. Front Genet. 2022;13: 977322.
16. Zhang G, Sun J, Zhang X. A novel Cuproptosis-related LncRNA signature to predict prognosis in hepatocellular carcinoma. Sci Rep. 2022;12(1):11325.
17. Ozben T, Ozben S. Neuro-inflammation and anti-inflammatory treatment options for Alzheimer's disease. Clin Biochem. 2019;72:87–9.
18. Ferrari C, Sorbi S. The complexity of Alzheimer's disease: an evolving puzzle. Physiol Rev. 2021;101(3):1047–81.
19. Weller J, Budson A. Current understanding of Alzheimer's disease diagnosis and treatment. F1000Res. 2018;7: F1000.
20. Chen L, Min J, Wang F. Copper homeostasis and cuproptosis in health and disease. Signal Transduct Target Ther. 2022;7(1):378.
21. Mangalmurti A, Lukens JR. How neurons die in Alzheimer's disease: implications for neuroinflammation. Curr Opin Neurobiol. 2022;75: 102575.
22. Cao X, Fu M, Bi R, Zheng X, Fu B, Tian S, et al. Cadmium induced BEAS-2B cells apoptosis and mitochondria damage via MAPK signaling pathway. Chemosphere. 2021;263: 128346.
23. Li Y, Chen F, Chen J, Chan S, He Y, Liu W, et al. Disulfiram/copper induces antitumor activity against both nasopharyngeal cancer cells and cancer-associated fibroblasts through ROS/MAPK and ferroptosis pathways. Cancers. 2020;12(1):138.
24. Muraleva NA, Stefanova NA, Kolosova NG. SkQ1 suppresses the p38 MAPK signaling pathway involved in Alzheimer's disease-like pathology in OXYS rats. Antioxidants. 2020;9(8):676.
25. Kim EK, Choi EJ. Pathological roles of MAPK signaling pathways in human diseases. Biochim Biophys Acta. 2010;1802(4):396–405.
26. Hirata H, Hinoda Y, Ueno K, Nakajima K, Ishii N, Dahiya R. MicroRNA-1826 directly targets beta-catenin (CTNNB1) and MEK1 (MAP2K1) in VHL-inactivated renal cancer. Carcinogenesis. 2012;33(3):501–8.
27. Ma Q, Zhao Y, Li Z, Gao W, Xu Y, Li B, et al. MicroRNA-34c-5p exhibits anti-cancer properties in gastric cancer by targeting MAP2K1 to inhibit cell proliferation, migration, and invasion. Biomed Res Int. 2022;2022:7375661.
28. Kim J, Lee HJ, Park SK, Park JH, Jeong HR, Lee S, et al. Donepezil regulates LPS and Aβ-stimulated neuroinflammation through MAPK/NLRP3 inflammasome/STAT3 signaling. Int J Mol Sci. 2021;22(19):10637.
29. Mi J, Luo J, Zeng H, Zhang H, Jamil M, Abdel-Maksoud MA, et al. Elucidating cuproptosis-related gene SLC31A1 diagnostic and prognostic values in cancer. Am J Transl Res. 2023;15(10):6026–41.
30. Lang M, Fan Q, Wang L, Zheng Y, Xiao G, Wang X, et al. Inhibition of human high-affinity copper importer Ctr1 orthologous in the nervous system of *Drosophila* ameliorates Aβ42-induced Alzheimer's disease-like symptoms. Neurobiol Aging. 2013;34(11):2604–12.
31. Zhu Y, Wu G, Yan W, Zhan H, Sun P. miR-146b-5p regulates cell growth, invasion, and metabolism by targeting PDHB in colorectal cancer. Am J Cancer Res. 2017;7(5):1136–50.
32. Wang H, Yang Z, He X, Guo F, Sun H, Xu S, et al. Cuproptosis related gene PDHB is identified as a biomarker inversely associated with the progression of clear cell renal cell carcinoma. BMC Cancer. 2023;23(1):804.
33. Colak D, Alaiya AA, Kaya N, Muiya NP, AlHarazi O, Shinwari Z, et al. Integrated left ventricular global transcriptome and proteome profiling in human end-stage dilated cardiomyopathy. PLoS ONE. 2016;11(10): e0162669.
34. Eskici G, Axelsen PH. Copper and oxidative stress in the pathogenesis of Alzheimer's disease. Biochemistry. 2012;51(32):6289–311.
35. Voss K, Harris C, Ralle M, Duffy M, Murchison C, Quinn JF. Modulation of tau phosphorylation by environmental copper. Transl Neurodegener. 2014;3(1):24.
36. Du X, Zheng Y, Wang Z, Chen Y, Zhou R, Song G, et al. Inhibitory act of selenoprotein P on Cu^{+}/Cu^{2+}-induced tau aggregation and neurotoxicity. Inorg Chem. 2014;53(20):11221–30.

Publisher's Note